

**Monomer-dimer reaction model with nearest-neighbor interactions at finite temperatures**

Vanessa S. Leite and Wagner Figueiredo\*

*Departamento de Física, Universidade Federal de Santa Catarina, 88040-900 Florianópolis, SC, Brazil*

(Received 03 June 2002; published 9 October 2002)

We studied a monomer-dimer catalytic surface reaction model of the type  $\frac{1}{2}A_2 + BA \rightarrow A_2B$ , where interactions between nearest-neighbor species and the temperature of the catalyst are considered. Through Monte Carlo simulations we determined the phase diagram of the model in the plane temperature versus partial pressure of the  $BA$  molecules in its gaseous phase. We found that the transition between the  $A$ -poisoned state and the active one is always continuous and the associated critical exponents are in the same universality class of the directed percolation (DP). On the other hand, the transition from the active state to the  $BA$ -poisoned one changes from continuous to first order for a given temperature value. The critical exponents of the continuous branch belong also to the DP universality class. For a small range of values of the partial pressure of  $BA$  and very low temperatures, we observe the formation of an inactive sublattice structure inside the active phase.

DOI: 10.1103/PhysRevE.66.046102

PACS number(s): 05.70.Ln, 82.65.+r, 05.70.Fh

**I. INTRODUCTION**

The subject of irreversible phase transitions has been used to describe a great variety of problems in physics, chemistry, and biology. However, the understanding of these phenomena is not complete, because we do not have at our disposal a closed formalism as in the equilibrium statistical mechanics. Aside from a few approximate analytical methods, such as the effective mean field theories, computational tools are very often used to get information on the irreversible processes. In general, these studies are performed for lattice models, which are suitable to be simulated by Monte Carlo methods. The book by Marro and Dickman [1] presents some examples of interacting particle systems on the lattice (contact process, catalysis models, lattice gases) where mean field theories and simulations are considered. An interesting class of problems that has been studied presents the so-called absorbing states. Once these states are reached by the system during its time evolution, the system cannot escape them anymore. The transition from active to absorbing states of a system is of great interest because different systems can exhibit the same universal character at the transition point.

In this work, we study a model where active and absorbing states are present. The model consists of the catalytic reaction  $\frac{1}{2}A_2 + BA \rightarrow A_2B$  occurring in a lattice at finite temperatures. We assume that nearest-neighbor adsorbed particles interact themselves. The interaction is considered repulsive for particles of the same species, and attractive for distinct sorts of particles. Not considering the temperature of the substrate or the interaction energy between adsorbed particles, this is similar to the well known Ziff-Gulari-Barshad (ZGB) model [2]. The ZGB model, is the simplest one used to explain the irreversible oxidation of CO molecules on a surface ( $\frac{1}{2}O_2 + CO \rightarrow CO_2$ ). In this model, the molecules of CO and  $O_2$  are deposited onto a square lattice, according to their partial pressures in the gaseous phase. The adsorption of CO molecules requires the existence of only one vacant

site, while the adsorption of  $O_2$  molecules needs two empty nearest-neighbor sites. Immediately after the adsorption of an  $O_2$  molecule, it dissociates and a reaction of oxidation can take place if a CO molecule is found in the neighborhood of each one of these free O atoms. The model presents two absorbing states, one poisoned by O atoms and the other poisoned by CO molecules. In between, an active state is present, and the transition from the active to the O-poisoned state is continuous, where the critical exponents associated with its transition point [3] put the ZGB model in the same universality class as the directed percolation (DP) [4]. On the other hand, the transition from the active to the CO-poisoned state is of the first-order type.

In order to consider more realistic models for surface problems in physics and chemistry, it would be interesting to include some lateral interactions between the adsorbed species [5–7]. Excluded-volume type interactions between nearest-neighbor particles may be interpreted as being due to their finite radius, which can be smaller or larger than the lattice parameter spacing. When the radius of an adsorbed reactant is larger than the lattice spacing, the lateral interactions work to inhibit the adsorption of a new particle in its neighborhood. On the other hand, when two nearest-neighbor particles are highly reactive, they like to stay closer to each other, and then an attractive interaction favors their nearest-neighbor adsorption.

For the model we are considering in this paper, where the temperature of the catalyst and the interactions between adsorbed particles are taken into account, we slightly changed the rules of the ZGB model, concerning the mechanisms of adsorption and reaction of the species. In the first place, for the adsorption process to occur, the existence of empty sites is not sufficient. For each trial of deposition, we calculate the energy change ( $\Delta E$ ) that this process would cause in the system. According to the above comments, we assume that the interaction energy between two identical nearest-neighbor adsorbed particles are repulsive, and we assigned the value  $+\varepsilon$  for this energy. Then, two  $A$  nearest-neighbor atoms or two nearest-neighbor  $BA$  molecules have the same energy. On the other hand, we assigned the value  $-\varepsilon$  for the interaction energy between an  $A$  atom and a  $BA$  molecule,

\*Email address: wagner@fisica.ufsc.br

when they are nearest neighbors in the square lattice. We disregarded the interaction between adsorbed species and the substrate. The substrate works only as a heat reservoir for the system. After calculating  $\Delta E$ , the deposition is accepted with probability one if  $\Delta E \leq 0$ , and with probability  $e^{-\Delta E/k_B T}$  if  $\Delta E > 0$  (here  $T$  is the temperature of the substrate, which is measured in units of  $\varepsilon/k_B$ , where  $k_B$  is the Boltzmann constant). Besides the energetics involved in the deposition of the molecules, there is a subtle difference between the deposition of an  $A_2$  molecule in our model and an  $O_2$  molecule in the ZGB model, even at very high temperatures. In the ZGB model, after choosing an empty site for the  $O_2$  deposition, the other site is randomly selected among the nearest-neighbor sites of the chosen site. It is possible that the new selected site is already occupied by an O or CO molecule, and in this case the adsorption of the  $O_2$  molecule is forbidden. In our model, after we chose the first site, the second one is looked for only among the empty neighboring sites of the first site. Concerning the reaction process between a pair of reactants  $A$  and  $BA$ , if more than one channel of reaction is opened after a given deposition, contrary to the usual random choice of ZGB model, here we attribute different weights to each channel according to the energy variation that it would cause to the system. In this way, the channels that cause the largest decrease in the energy of the system are more probable.

With this model in mind, we performed extensive Monte Carlo simulations, and we determined its phase diagram in the plane  $T$  versus  $y_{BA}$ , where  $y_{BA}$  is the partial pressure of the  $BA$  molecules in the gaseous mixture. We also have calculated the static critical exponents for the continuous branches of the phase diagram, and we built hysteresis curves for the first-order phase transitions. Models including lateral interactions between nearest-neighbor particles have already been studied. Satulovsky and Albano [8] determined the phase diagram for this model and for other choices of the energy couplings between the adsorbed particles. While Satulovsky and Albano focused their attention on the phase diagram for a variety of couplings between particles, in our model we chose a particular set of parameters studied by these authors, and we paid special attention to the details of the observed phase transitions. One-dimensional versions of the model were previously studied [9–11] where only infinite repulsive lateral interactions between identical adsorbed monomers were considered. In the absence of a symmetry breaking field, these models belong to a different universality class from directed percolation (DP), called directed Ising (DI) universality class. These models present two equivalent poisoned states, which mimic the degenerate ground state of the Ising model. Monetti [12] considered the same one-dimensional model, but from a different perspective, where the lateral interactions were of finite magnitude. In this way, he found a reactive window for suitable values of the interaction parameter.

The remainder of this paper is organized as follows: In Sec. II, we describe the Monte Carlo simulations; in Sec. III we present the phase diagram of this model, Sec. IV contains a detailed analysis of the phase transitions, and in the last section, we summarize the results.

## II. MONTE CARLO SIMULATIONS

We have performed simulations for this catalytic reaction model on a square lattice with linear dimensions ranging from  $L=8$  to  $L=128$ . We started all simulations with an empty lattice (save in the cases where we were investigating the existence of hysteresis loops in the first-order transitions) and used periodic boundary conditions. In all simulations the temperature was measured in units of  $\varepsilon/k_B$ .

For each value of temperature and of the deposition rate of  $BA$  molecules,  $y_{BA}$ , we generate a random number to determine what molecule we will try to deposit in the next step. If we choose  $BA$ , we generate another random number to select an empty site for its adsorption. Then we calculate the change in the energy ( $\Delta E$ ) of the system that the deposition in this selected site would cause. If  $\Delta E \leq 0$ , the molecule is immediately adsorbed. In the case where  $\Delta E > 0$ , the adsorption is accepted with probability  $e^{-\Delta E/k_B T}$ . If the chosen molecule is  $A_2$ , we again select at random an empty lattice site. Then, for each one of its empty neighbors (if they exist), we calculate the energy change that the deposition of an  $A$  atom on it would cause to the system. We attribute a larger weight for that neighbor with smaller  $\Delta E$ . After we have defined the pair of nearest-neighbor sites, then we calculate  $\Delta E$  corresponding to the deposition of  $A_2$ . Again, if  $\Delta E \leq 0$ , the molecule is adsorbed, and if  $\Delta E > 0$ , it is adsorbed with probability  $e^{-\Delta E/k_B T}$ .

For both molecules, after a successful deposition trial, we have to investigate the neighborhood of the adsorbed species to look for possible reactions. If there is no possibility of reaction, the molecule remains adsorbed in the lattice. If there is only a single possible reaction channel, it occurs immediately. Finally, if more than one reaction channel is opened, we calculate the energy change that each reaction would cause in the system, and we assign a larger probability for the choice that most decreases the energy of the system. Then, after the choice of the reactants, the reaction occurs immediately, leaving two new empty sites in the lattice.

## III. PHASE DIAGRAM

We show in Fig. 1 a typical coverage diagram obtained for a lattice with  $L=128$  at high temperatures. For this plot we have  $T=10^4$ , and in this case, the probability  $e^{-\Delta E/k_B T} \rightarrow 1$ , that is, the probability of deposition of particles depends only on the presence of empty sites in the lattice. This diagram is very similar to the one found in the work of Ziff, Gulari, and Barshad [2]. However, while in our model the transition between the  $A$ -poisoned and active states occurs at  $y_1 \approx 0.62$ , in the ZGB model this transition occurs at  $y_1 \approx 0.39$ . Also, for the first-order transition between the active and  $BA$ -poisoned states, we found  $y_2 \approx 0.65$ , while the corresponding value in the ZGB model is  $y_2 \approx 0.52$ . Then, the reactive window in our model at high temperatures is narrower than in the ZGB model. The difference between these models is related to the way we consider the process of adsorption of  $A_2$  molecules. Our model, at high temperatures, favors the  $A_2$  adsorption more than in the ZGB model. When we select the first site for the deposition of the molecule, if

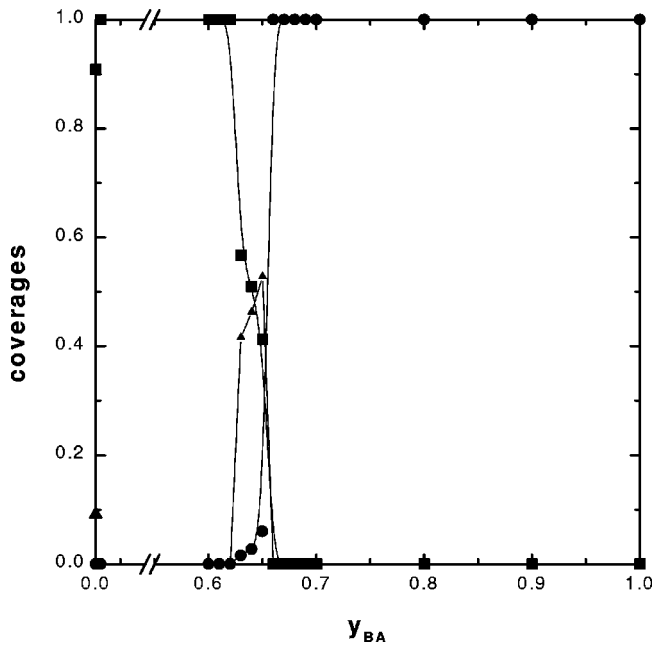


FIG. 1. Coverages of the lattice for  $L=128$  as a function of  $y_{BA}$  at temperature  $T=10^{-4}$ . Squares,  $n_A$ ; triangles,  $n_V$ ; circles,  $n_{BA}$ . The lines serve as a guide to the eyes.

one of its nearest-neighbor sites is empty, the deposition always occurs. This rule does not apply to the ZGB model, since the choice of the second site for the deposition is made randomly, and eventually one occupied site can be chosen, forbidding the adsorption.

Figure 2 exhibits a representative coverage diagram at very low temperatures. For these temperatures, the Boltzmann's weight,  $e^{-\Delta E/k_B T} \rightarrow 0$ , always we try to deposit one

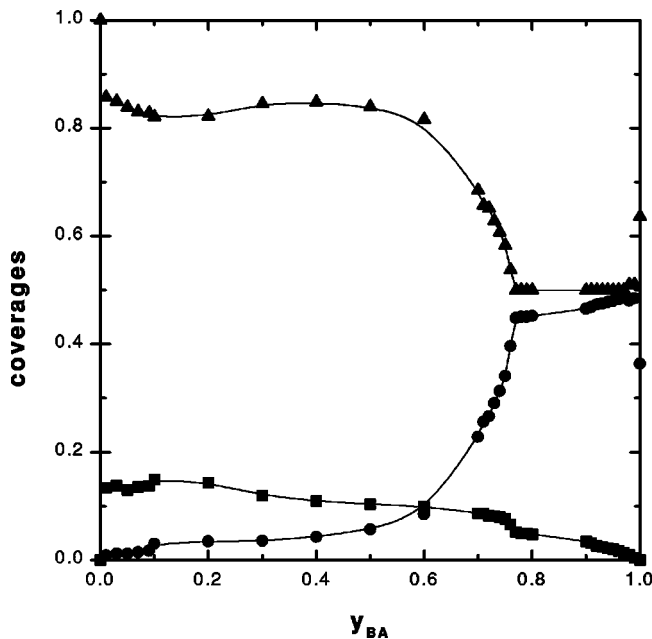


FIG. 2. Coverages of the lattice for  $L=128$  as a function of  $y_{BA}$  at temperature  $T=10^{-4}$ . Squares,  $n_A$ ; triangles,  $n_V$ ; circles,  $n_{BA}$ . The lines serve as a guide to the eyes.

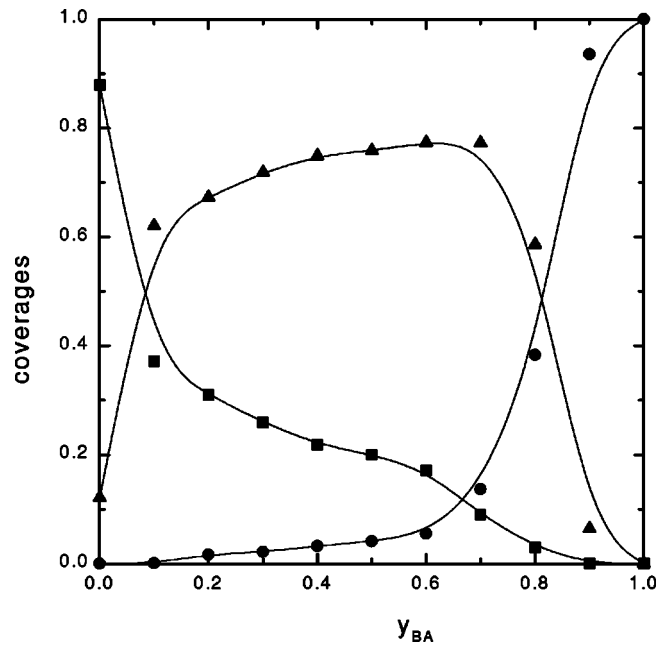


FIG. 3. Coverages of the lattice for  $L=128$  as a function of  $y_{BA}$  at temperature  $T=0.5$ . Squares,  $n_A$ ; triangles,  $n_V$ ; circles,  $n_{BA}$ . The lines serve as a guide to the eyes.

molecule that increases the energy of the system. Then, at these temperatures, the catalyst has a large density of empty sites for any value of the deposition rate  $y_{BA}$ . In particular, for large values of  $y_{BA}$ , we observe a chessboard formation: one sublattice is formed by blank sites, and the other is formed predominantly by  $BA$  molecules. Then, in this range of values of  $y_{BA}$ , and at very low temperatures, the catalyst is inactive.

At intermediate temperature values, we obtained coverage diagrams like that of Fig. 3. The structure of sublattices is lost, and the reactive window appears for all values of the deposition rate of  $BA$  molecules.

Finally, in Fig. 4 we show the complete phase diagram in the plane  $T$  versus  $y_{BA}$  for this model. We note the existence of four distinct regions: an  $A$ -poisoned, a  $BA$ -poisoned, an active, and a chessboard, which is seen in the inset of Fig. 4. As we will see in the following section, the phase transition between the  $A$ -poisoned and active states is continuous, while the phase transition between the active and  $BA$ -poisoned states is continuous at low temperatures and first order at high temperatures. Besides, the phase transition between the active and chessboard states is of the first-order type.

#### IV. PHASE TRANSITIONS

In the last section we showed the phase diagram of the model, where four distinct regions appear. In this section, we will focus our attention on the study of the phase transitions between the different regions of the phase diagram. In the following, we will illustrate these transitions by choosing some points of the phase diagram and considering the behavior of the order parameter, which in our case is the fraction of empty sites, in the neighborhood of these points.

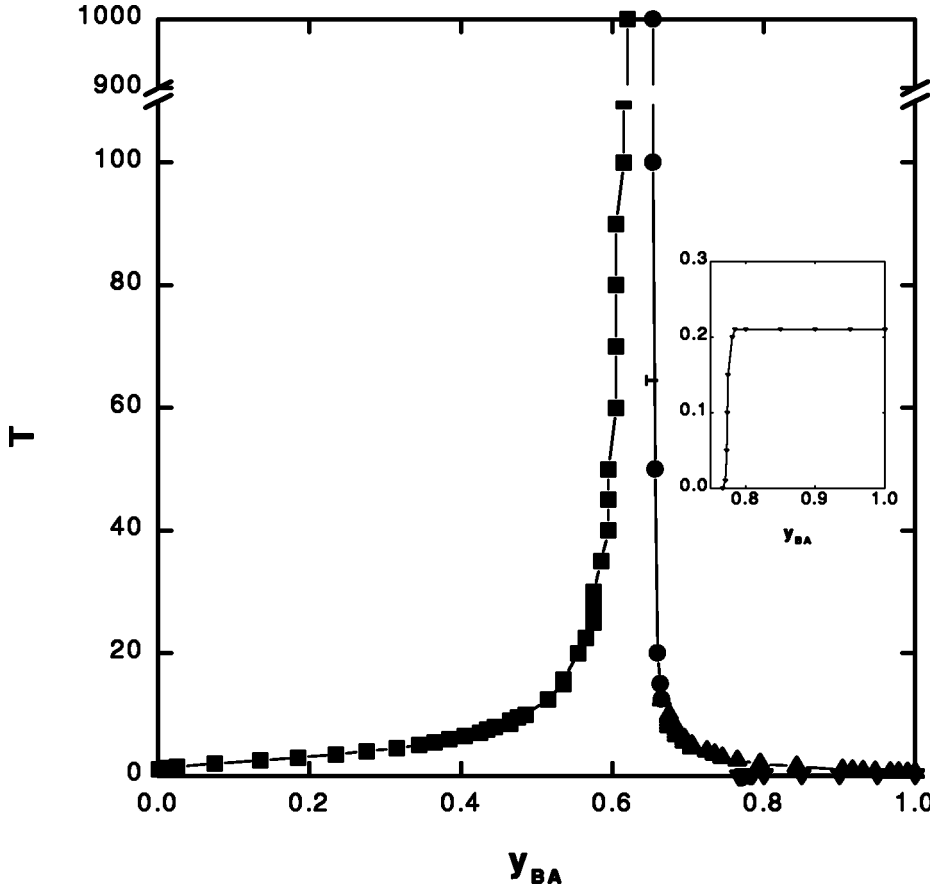


FIG. 4. Phase diagram in the plane  $T$  (measured in units of  $\epsilon/k_B$ ) versus  $y_{BA}$ . At the left side we have the  $A$ -poisoned state, at the right side we have the  $BA$ -poisoned state, the center of the diagram represents the active states of the model, and in the inset we display the region corresponding to the chessboard state.

Let us first consider the phase transition between the  $A$ -poisoned and active states of the system. In the ZGB model, this transition is always continuous, and belongs to the DP universality class [4]. In order to study this transition in our model, we fixed the temperature of the substrate and we swept the values of the deposition rate of  $BA$  molecules  $y_{BA}$  around the transition point, for that temperature. A preliminary analysis based on the coverage diagrams, showed that the order parameter (density of empty sites  $n_V$ ) changes continuously through the transition.

To find the critical point of this transition, we used the same methods employed by us in a previous paper [3] to determine the critical point of the ZGB model. We considered the stationary values of the order parameter for different lattice sizes in the vicinity of the critical point. The order parameter obeys the scaling relation

$$n_V(\Delta, L) \propto L^{-\frac{\beta}{\nu_\perp}} f\left(\Delta L^{\frac{1}{\nu_\perp}}\right), \quad (1)$$

where  $\Delta = y_{BA} - y_1$ ,  $y_1$  is the critical point for the lattice of infinite size, and the scaling function  $f(x) \propto x^\beta$  for large values of  $x$ .  $\beta$  is the order parameter critical exponent and  $\nu_\perp$  is the critical exponent associated with the spatial correlation length. At the critical point this equation can be written as

$$n_V(0, L) \propto L^{-\frac{\beta}{\nu_\perp}}. \quad (2)$$

Therefore, through log-log plots of the density  $n_V$  versus  $L$ , we can find the critical point, which corresponds to the

straight line behavior. For instance, Fig. 5 shows the log-log plot of  $n_V$  versus  $L$  for the temperature  $T=1.25$  and five different values of the deposition rate  $y_{BA}$ . From this plot, the data points that best fit the power law of Eq. (2) correspond to a critical value of  $y_1 = 0.0120 \pm 0.0002$ , the central curve in the plot of Fig. 5. From adjusting the points of this central curve to a straight line, we find that the ratio between the critical exponents is  $(\beta/\nu_\perp) = 0.81 \pm 0.01$ . The curves associated with the simulation points corresponding to  $y_{BA} = 0.0115$  and  $y_{BA} = 0.0125$  already exhibit a concave and a convex behavior, respectively. We also can estimate the critical exponents  $\beta$  and  $\nu_\perp$  through the collapse of the data for all lattices. We have plotted in Fig. 6  $n_V L^{\beta/\nu_\perp}$  versus  $\Delta L^{1/\nu_\perp}$  in a log-log scale. As we can see, the data for different lattice sizes collapse very well, suggesting the correctness of the scaling form of Eq. (1). Thus, for large values of the argument of the function  $f(x)$  in Eq. (1), the data in Fig. 6 should fall on a line with slope  $\beta$ . The collapse of the data points was obtained with the following values of the parameters:  $\beta = 0.60$ ,  $\nu_\perp = 0.74$  and  $y_1 = 0.0120$ . We observe that the ratio  $\beta/\nu_\perp$  is the same as the one seen in Fig. 5. These critical exponents appear to be in very close agreement with those of the DP. The best values for the critical exponents of the directed percolation in (2+1) dimensions are [13]  $\beta = 0.584(4)$  and  $\nu_\perp = 0.734(4)$ .

Further support for the idea that the transition between  $A$ -poisoned and active states is in the DP universality class comes from the analyses of the moment ratios of the order parameter at the critical point. As in our previous paper [3],

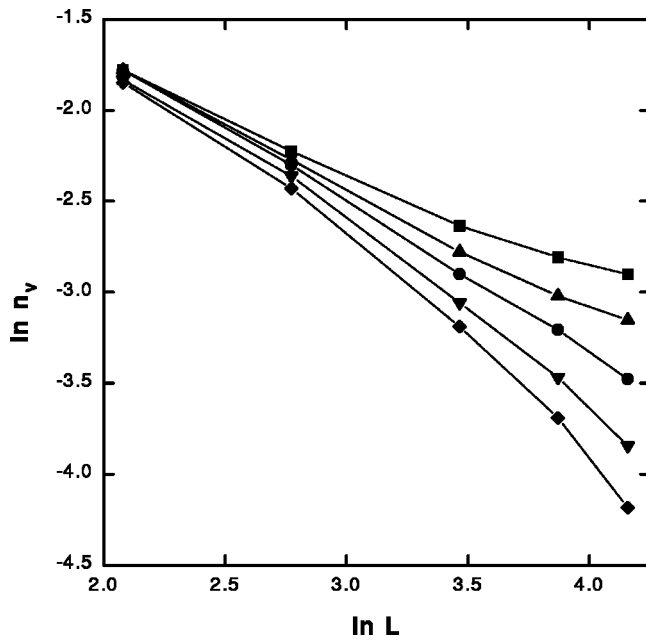


FIG. 5. Stationary density of vacant sites  $n_V$  versus system size  $L$  for  $y_{BA} = 0.0110, 0.0115, 0.0120, 0.0125,$  and  $0.0130$  (from bottom to top) at temperature  $T = 1.25$ . The lines serve to guide the eyes. The critical point is determined by adjusting the central curve to a straight line.

we calculate some ratios between the moments of the order parameter. For instance, we considered all moments up to fourth order, defined by  $m_k = \langle n_V^k \rangle$ , with  $k = 1, 2, 3, 4$ , and also the second-order cumulant,  $Q_2 = m_2 - m_1^2$ . Then, we formed the following ratios:  $Q_2/m_1^2$ ,  $m_4/m_2^2$ ,  $m_3/m_1^3$ ,  $m_3/m_1 m_2$  and  $m_2/m_1^2$ . At the critical point, these ratios are independent

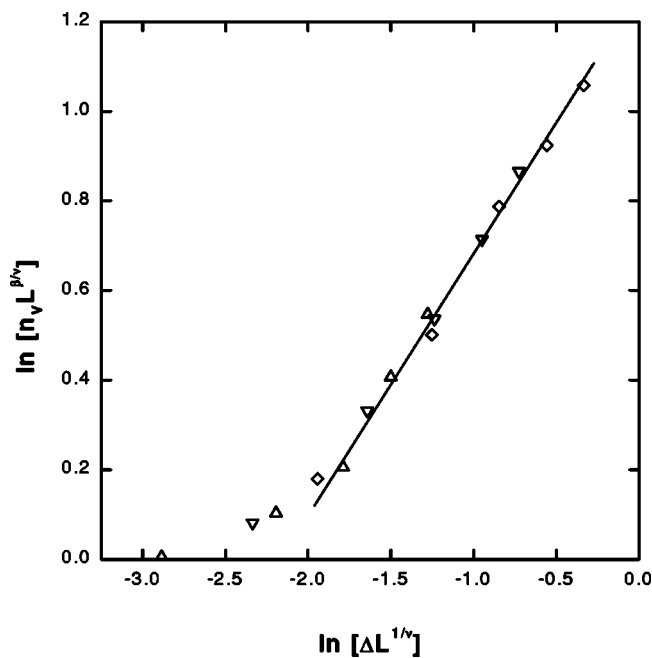


FIG. 6. Log-log plot of  $n_V L^{\beta/\nu_\perp}$  versus  $\Delta L^{1/\nu_\perp}$  in the neighborhood of the critical point  $y_{BA} = 0.0120$  at temperature  $T = 1.25$ . Up triangles,  $L = 16$ , down triangles,  $L = 32$ , diamonds,  $L = 64$ .

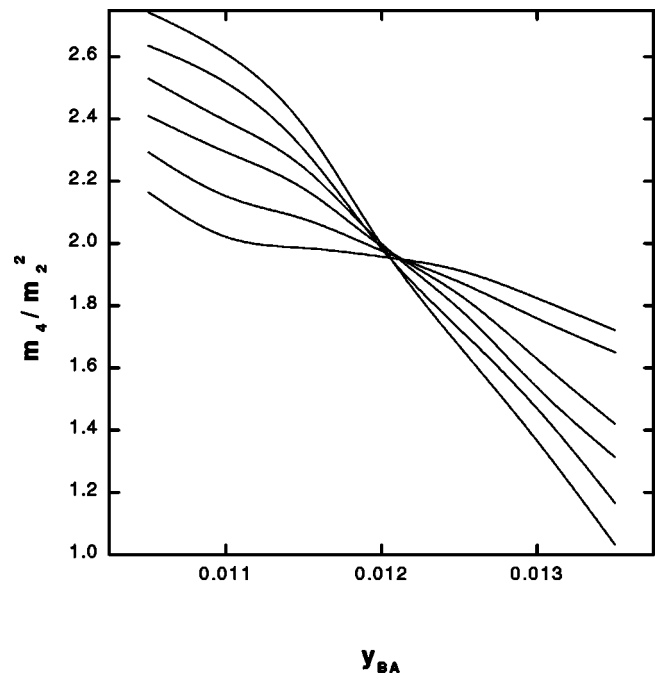


FIG. 7. Ratio  $m_4/m_2^2$  versus  $y_{BA}$  at temperature  $T = 1.25$ . System sizes  $L = 8, 16, 32, 48, 64,$  and  $128$  are in order of increasing steepness.

of the lattice size [1]. In this way, we expect that plots of these ratios, as a function of  $y_{BA}$ , must intercept themselves at the critical point for any value of the lattice size  $L$ .

Figures 7 and 8 depict this behavior for the ratios  $m_4/m_2^2$  and  $m_3/m_1 m_2$  versus  $y_{BA}$  for  $T = 1.25$ , respectively. From these figures, we clearly see that the ratios are independent of  $L$  at  $y_{BA} = y_1$ . In Fig. 9 we summarize the results obtained

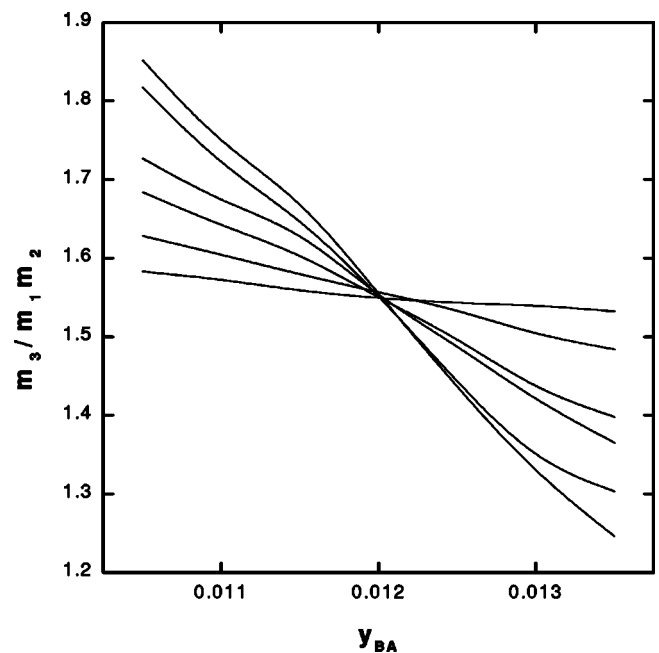


FIG. 8. Ratio  $m_3/m_1 m_2$  versus  $y_{BA}$  at temperature  $T = 1.25$ . System sizes  $L = 8, 16, 32, 48, 64,$  and  $128$  are in order of increasing steepness.

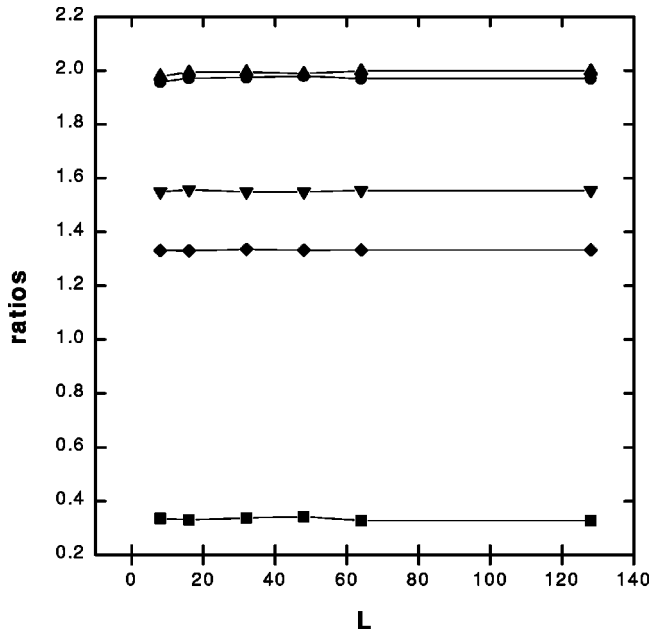


FIG. 9. Order-parameter moment ratios at the critical point and at temperature  $T=1.25$ . Squares,  $Q_2/m_1^2$ ; diamonds,  $m_2/m_1^2$ ; down triangles,  $m_3/m_1m_2$ ; up triangles,  $m_3/m_1^3$ ; circles,  $m_4/m_2^2$ .

for all the moment ratios at the critical point. By a suitable linear extrapolation of these ratios to  $L \rightarrow \infty$  we obtained the values  $Q_2/m_1^2=0.328$ ,  $m_4/m_2^2=1.972$ ,  $m_3/m_1^3=1.998$ ,  $m_3/m_1m_2=1.554$ , and  $m_2/m_1^2=1.333$ , which are in close agreement with those found for the ZGB model [3], the contact process [14] and also for the pair contact process [15] in two dimensions. As we pointed out before, these results corroborate the idea that these models belong to the DP universality class.

All the previous analyses were made for the particular value  $T=1.25$ . Indeed, we have performed the same kind of investigation for other temperature values along the line of transition between the  $A$ -poisoned and active states. We have seen that the transition line is always continuous, and the calculated critical exponents and moment ratios clearly put this transition in the same universality class of the DP.

Let us turn to the phase transition between the active and the  $BA$ -poisoned states. After doing a detailed investigation for different temperature values along the transition line, we observed that the transition changes from continuous to first order at the temperature  $T=12.9$ . For the branch of the transition line where the transition is discontinuous, the hysteresis curves exhibit a well defined loop [16,17]. For example, we illustrate in Fig. 10 a kind of hysteresis loop observed for temperatures  $T>12.9$ . The branches of the loop are obtained by starting the simulations at different initial conditions. As a matter of comparison, Fig. 11 shows the same kind of plot as in Fig. 10, but for  $T=12.9$ . We see that the loop disappears at this temperature. Indeed, for all values of temperature  $T \leq 12.9$ , there are no more loops, and the transition is always continuous. In order to study the critical behavior in this portion of the transition line, we used the same tools employed in the transition between the  $A$ -poisoned and active states. We do not repeat all the procedures here, but we have

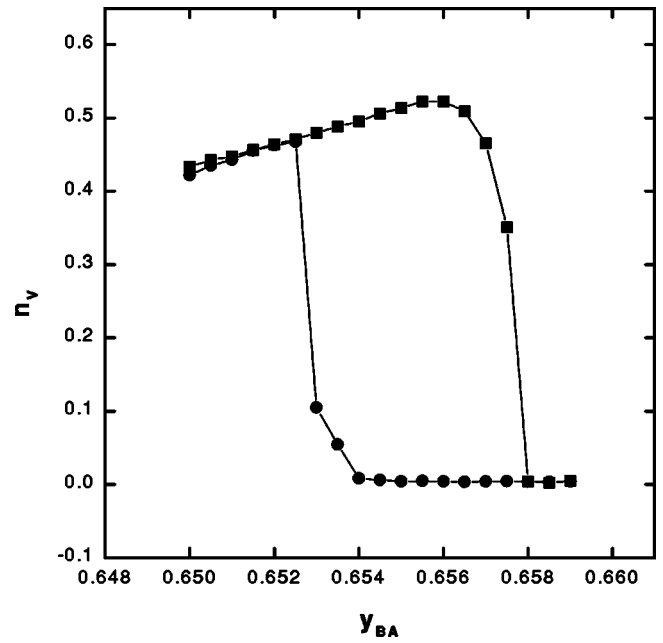


FIG. 10. Hysteresis curve obtained at temperature  $T=2000$  in the transition between the active and  $BA$ -poisoned states. The squares represent the results found for simulations starting with an empty lattice, and the circles for an initially half-filled lattice.

verified that the critical exponents and the moment ratios determined along this portion of the transition line show that this line of critical points is in the same universality class of the DP.

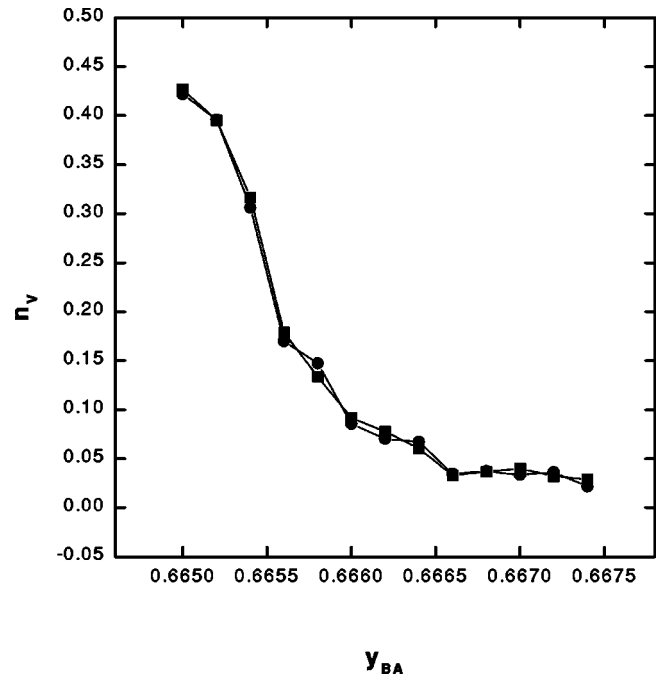


FIG. 11. Stationary density of vacant sites  $n_v$  versus  $y_{BA}$  in the neighborhood of the transition between the active and  $BA$ -poisoned states, at temperature  $T=12.9$ . Hysteresis loop is not observed at this temperature. The squares represent the results found for simulations starting with an empty lattice, and the circles for an initially half-filled lattice.

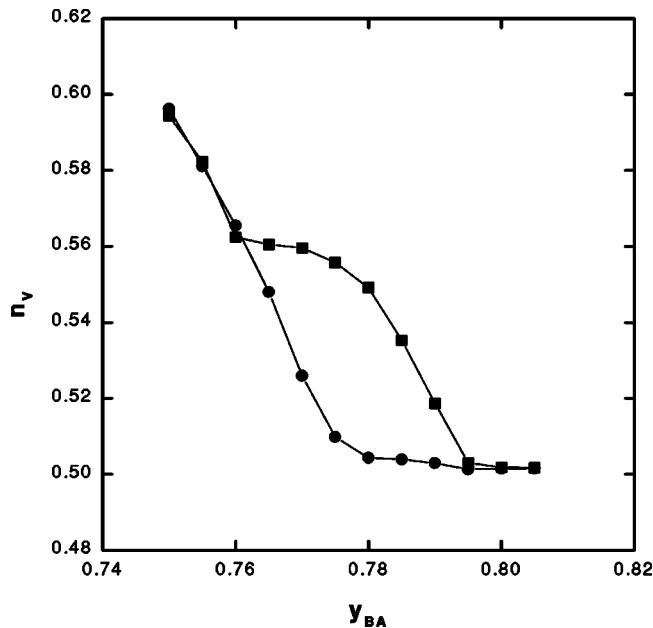


FIG. 12. Hysteresis curve obtained at temperature  $T=0.1$  in the transition between the active and the chessboard states. The squares represent the results found for simulations starting with an empty lattice, and the circles for an initially half-filled lattice.

Let us mention the type of results we found for the transition between the active and chessboard states at very low temperatures. We have built hysteresis curves for several points at the transition line. Figure 12 is an example of the behavior observed at the temperature  $T=0.1$ , where a loop is clearly identified. This kind of picture is observed for all values of temperature at this transition line. Therefore, the transition between the active and chessboard states is always of the first-order type.

## V. CONCLUSIONS

We have studied a monomer-dimer model with lateral interactions between the adsorbed particles at finite temperatures of the catalyst. At high temperatures the model can be seen as a variant of the ZGB model, where the dimer absorption process is favored. Then, at these temperatures, this model shows a smaller reactive window than that observed in the ZGB model. Through extensive Monte Carlo simulations we determined the phase diagram of the model in the plane temperature versus partial pressure of the  $BA$  molecules in its gaseous phase. We found that the width of the reactive window increases as we lower the temperature. However, at very low temperatures and for a small range of values of the deposition rate of  $BA$  molecules, we observed the formation of a structure of sublattices where the catalyst becomes inactive.

The phase diagram presents four distinct regions:  $A$ - and  $BA$ -poisoned regions, an active and a chessboard inactive region. We have determined the nature of the phase transitions between the different regions of the diagram. For this purpose, we have used hysteresis curves, moment ratios, and finite size arguments. We have shown that the transition line between the  $A$ -poisoned and active states is a line of critical points that belongs to the DP universality class. On the other hand, the transition line between the active and  $BA$ -poisoned states is continuous at low temperatures and belongs to the DP universality class, too, and turns into a first-order transition line at high temperatures. Finally, we have seen that the transition line that separates the active and chessboard regions is always of the first order.

## ACKNOWLEDGMENTS

This work was supported by the Brazilian agencies CAPES and CNPq.

- 
- [1] J. Marro and R. Dickman, *Nonequilibrium Phase Transitions in Lattices Models* (Cambridge University Press, Cambridge, 1999).
  - [2] R.M. Ziff, E. Gulari, and Y. Barshad, *Phys. Rev. Lett.* **56**, 2553 (1986).
  - [3] V.S. Leite, G.L. Hoenicke, and W. Figueiredo, *Phys. Rev. E* **64**, 036104 (2001).
  - [4] G. Grinstein, Z.-W. Lai, and Dana A. Browne, *Phys. Rev. A* **40**, 4820 (1989).
  - [5] H.P. Kaukonen and M. Nieminen, *J. Chem. Phys.* **91**, 4380 (1989).
  - [6] F. Bagnoli, B. Sente, M. Dumont, and R. Dagonnier, *J. Chem. Phys.* **94**, 777 (1991).
  - [7] J.J. Luque, F. Jiménez-Morales, and M.C. Lemos, *J. Chem. Phys.* **96**, 8535 (1992).
  - [8] J. Satulovsky and E.V. Albano, *J. Chem. Phys.* **97**, 9440 (1992).
  - [9] M.H. Kim and H. Park, *Phys. Rev. Lett.* **73**, 2579 (1994).
  - [10] H. Park, M.H. Kim, and H. Park, *Phys. Rev. E* **52**, 5664 (1995).
  - [11] H. Park and H. Park, *Physica A* **221**, 97 (1995).
  - [12] R.A. Monetti, *Phys. Rev. E* **58**, 144 (1998).
  - [13] H. Hinrichsen, *Adv. Phys.* **49**, 815 (2000).
  - [14] R. Dickman and J. Kamphorst Leal da Silva, *Phys. Rev. E* **58**, 4266 (1998).
  - [15] J. Kamphorst Leal da Silva and R. Dickman, *Phys. Rev. E* **60**, 5126 (1999).
  - [16] J.W. Evans and M.S. Miesch, *Phys. Rev. Lett.* **66**, 833 (1991).
  - [17] R.A. Monetti and E.V. Albano, *J. Phys. A* **34**, 1103 (2001).